Auger Recombination in Sodium-Iodide scintillators From First Principles

A. McAllister, D. Aberg, A. Schleife, E. Kioupakis

January 12, 2015

Disclaimer

This document was prepared as an account of work sponsored by an agency of the United States government. Neither the United States government nor Lawrence Livermore National Security, LLC, nor any of their employees makes any warranty, expressed or implied, or assumes any legal liability or responsibility for the accuracy, completeness, or usefulness of any information, apparatus, product, or process disclosed, or represents that its use would not infringe privately owned rights. Reference herein to any specific commercial product, process, or service by trade name, trademark, manufacturer, or otherwise does not necessarily constitute or imply its endorsement, recommendation, or favoring by the United States government or Lawrence Livermore National Security, LLC. The views and opinions of authors expressed herein do not necessarily state or reflect those of the United States government or Lawrence Livermore National Security, LLC, and shall not be used for advertising or product endorsement purposes.

Auger recombination in sodium-iodide scintillators from first principles

Andrew McAllister,[1] Daniel Åberg,[2] André Schleife,[3] and Emmanouil Kioupakis[4, a)]

[1)] *Applied Physics Program, University of Michigan, Ann Arbor, Michigan 48109, USA*

[2)] *Physical and Life Sciences Directorate, Lawrence Livermore National Laboratory, Livermore, California 94550, USA*

[3)] *Department of Materials Science and Engineering, University of Illinois at Urbana-Champaign, Urbana, Illinois 61801, USA*

[4)] *Department of Materials Science and Engineering, University of Michigan, Ann Arbor, Michigan 48109, USA*

(Dated: 15 December 2014)

Scintillator radiation detectors suffer from low energy resolution that has been attributed to non-linear light yield response to the energy of the incident gamma rays. Auger recombination is a key non-radiative recombination channel that scales with the third power of the excitation density and may play a role in the nonproportionality problem of scintillators. In this work we study direct and phonon-assisted Auger recombination in NaI with first-principles calculations. Our results show that phonon-assisted Auger recombination, mediated primarily by short-range phonon scattering dominates at room temperature. We discuss our findings in light of the much larger values obtained by numerical fits to z-scan experiments.

PACS numbers: 72.20.Jv, 71.20.Nr, 71.15.Qe, 78.70.Ps, 29.40.Mc

Scintillator devices based on sodium iodide (NaI) are used in national security to enable simple and fast scanning for radioactive materials in shipping containers at ports or on trucks. Scintillators convert high-energy gamma rays into photons of lower energy [Fig. 1(a)] that are easier to analyze using, e.g., optoelectronic devices, to identify the elemental source of detected gamma radiation.

Unfortunately, current scintillator materials including NaI suffer from low energy resolution that leads to high false-alarm rates for materials such as ceramics or cat litter that are not considered a severe threat.[1,2] These false-positives can be offset by additional instrumentation, which, however, leads to increased cost and complexity of the scanning system. A number of recent studies investigated the non-proportionality effect in order to improve the accuracy of scintialtor detectors (Refs. 3–11).

One dissipative process that may play a role in scintillator nonproportionality is Auger recombination (AR). *Direct* AR takes place when an electron and hole recombine non-ratiatively to excite a third carrier instead of radiating a photon [Fig. 1(b) and (c)]. *Indirect* AR occurs when the non-radiative recombination process is assisted by a carrier-scattering mechanism that provides additional momentum, e.g., a phonon [Fig. 1(d)]. The AR rate R_{Auger} is proportional to the third power of the free-carrier density n, and the Auger coefficient C is defined as $R_{\mathrm{Auger}} = Cn^3$.[12] A comparison with the radiative recombination rate, which increases with the square of the free-carrier density, $R_{\mathrm{rad}} = Bn^2$, shows that AR dominates at high carrier densities. AR is thought to reduce

———
a)Electronic mail: kioup@umich.edu

the high-power efficiency of light emitting diodes[13,14] and may also play a role in the non-proportionality problem of scintillators.[15] In all of these cases, understanding the microscopic mechanism of AR is a prerequisite to improving the device performance.

There is no theoretical and very little experimental data regarding AR in NaI. Experimental measurements of AR in scintillators are extremely difficult, since each incident gamma-ray photon generates multiple carriers, which can interact through several non-radiative mechanisms that are impossible to discern directly. The analysis of experimental data must then try to relate properties such as the light yield to models that include AR rate parameters. However, different experimental condictions and underlying assumptions used in models can lead to AR coefficients spanning many orders of magnitude. Using rate equations for the temporal and spatial evolution of excitation densities, the work in Ref. 8 found an AR coefficient of 1.07×10^{-20} cm^{6}s^{-1} when modeling Compton coincidate data from SLYNCI (see Ref. 5). On the other hand, a much smaller coefficient of 3.2×10^{-29} cm^{6}s^{-1} was reported when modeling z-scan experiments using a pulsed laser.[16,17] These few data points span nine orders of magnitude and emphasize the need for first-principles studies of AR in scintillators to thoroughly understand the involved processes and provide complementary and independent insight without empirical assumptions.

In this work, we investigate direct and phonon-assisted AR in sodium iodide, a widely used and well characterized scintillating material, using first-principles calculations based on density functional theory. We show that AR is dominated by the phonon-assisted process and is primarily mediated by short-range acoustic and longitudinal optical phonons. From our computations we derive values of $1.17 \pm 0.01 \times 10^{-33}$ cm^{6}s^{-1} for the direct and $5.6 \pm 0.3 \times 10^{-32}$ cm^{6}s^{-1} for the phonon-assisted AR co-
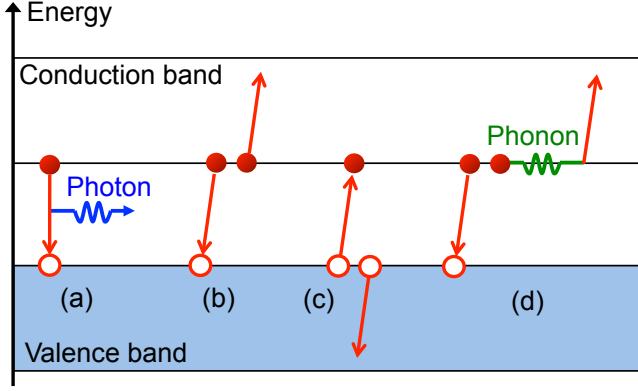
FIG. 1. Schematic illustration of recombination processes in scintillators after a high-energy impact. (a) Radiative recombination of an electron-hole pair produces a photon. (b)-(c) In non-radiative Auger recombination the energy of the recombining pair is transferred to a third carrier, either (b) an electron (e-e-h Auger) or (c) a hole (h-h-e Auger) that gets excited to a higher energy state. (d) Auger recombination can also be mediated by a phonon.
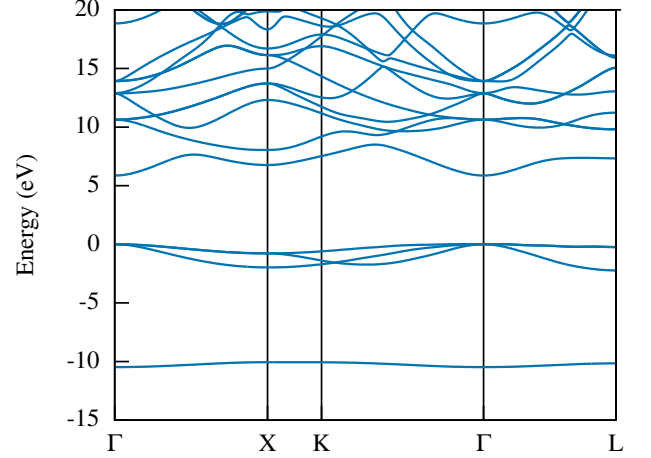

FIG. 2. The calculated band structure of NaI. Energies are referenced to the valence band maximum at Γ. The gap has been rigidly adjusted to the experimental value (5.8 eV) to account for the band gap problem of density functional theory. The absence of valence bands around –5.8 eV indicates that h-h-e Auger process [Fig. 1(c)] is not possible in this material.
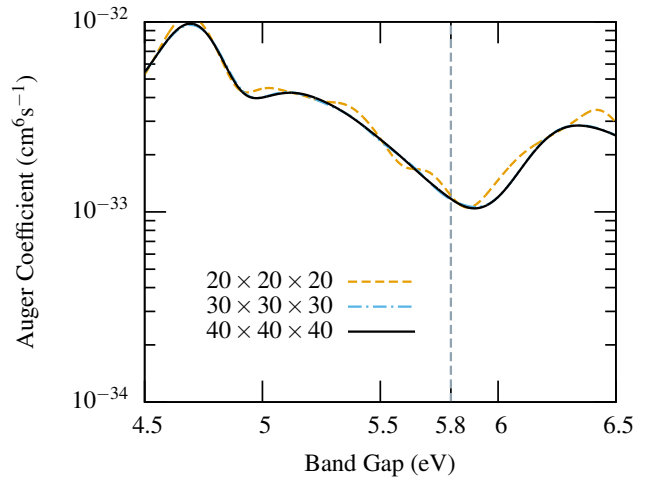

FIG. 3. Calculated values for the direct e-e-h Auger recombination coefficient of NaI as a function of the grid spacing used to sample the BZ and the (rigidly adjusted) band gap of the material. The converged value for the experimental band gap is $1.17 \pm 0.01 \times 10^{-33}$ cm^{6}s^{-1}.

efficient. Our analysis shows that direct AR follows an Arrhenius activation law and cannot exceed the phonon-assisted AR rate even at high electronic temperatures.

Our computational methodology is based on density functional theory (DFT) in the generalized gradient approximation[18] and the plane-wave norm-conserving pseudopotential method.[19–21] The calculated direct gap was rigidly adjusted to the experimental value[22] (E_g=5.8 eV) to account for the band-gap problem of DFT. Spin-orbit interaction effects were not included in the calculations. The maximally localized Wannier function method[23,24] was used to interpolate the energy bands to fine grids in the first Brillouin zone (BZ). Direct and phonon-assisted AR rates were calculated as described in Refs. 13 and 25. Gaussian functions with a width of 0.1 eV were used to evaluate the energy delta functions for the AR rates. We used a model dielectric function[26] to calculate the screened Coulomb interaction matrix elements, including the screening by free carriers using the Debye-Hückel equation for non-degenerate carriers and the Thomas-Fermi model for degenerate carrier concentrations.[12] The lattice temperature is taken to be 300 K while the electron temperature is set to 500 K. We assume a carrier density of 10^{19} cm^{-3}. We use a lattice constant of 12.58 Bohr radii and the experimental high frequency dielectric constant $\epsilon_\infty = 2.98$.

Figure 2 shows the calculated band structure of NaI. AR excites carriers to states that are at energies approximately equal to the band gap from the conduction and valence-band edges. As is evident from the band structure in Fig. 2 there are numerous conduction bands at the energy ($2E_g$=11.6 eV) needed to accommodate hot electrons excited by the e-e-h Auger process [Fig. 1(b)]. Thus we conclude that direct and phonon-assisted e-e-h

AR are possible in NaI. However, there are no valence-band states around −5.8 eV to accommodate holes excited by the h-h-e Auger process [Fig. 1(c)] and therefore h-h-e AR cannot occur in NaI. In the following, we focus our attention to e-e-h Auger processes only.

The calculated values for the direct e-e-h AR coefficients are shown in Fig. 3. To estimate the sensitivity of the calculated coefficients to the band gap value we adjusted the value of the band gap between 4.5−6.5 eV. The calculated value at the experimental band gap is $1.17 \pm 0.01 \times 10^{-33}$ cm^{6}s^{-1}. Figure 3 shows that a BZ
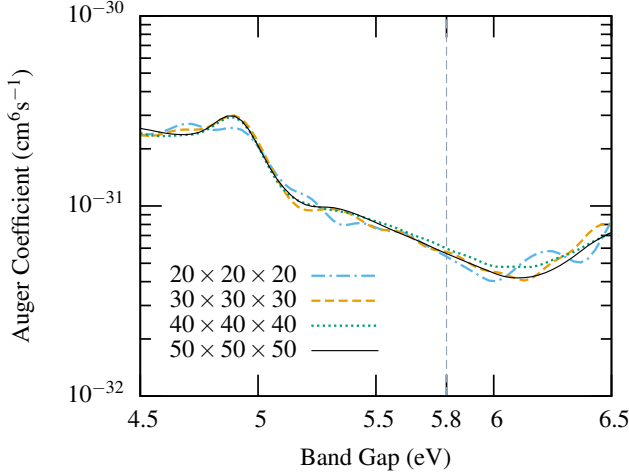
FIG. 4. Calculated phonon-assisted e-e-h Auger recombination coefficients of NaI as a function of the adjusted band gap and the BZ sampling. The phonon-assisted Auger coefficient at the experimental band gap value is $5.6 \pm 0.3 \times 10^{-32}$ cm^{6}s^{-1}, which is approximately two orders of magnitude larger than the direct Auger coefficient (cf. Fig. 3).
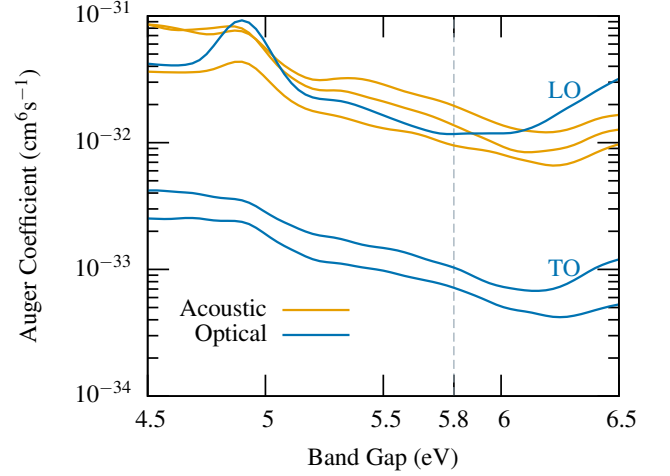

FIG. 5. The contribution of the various phonon modes to the phonon-assisted Auger coefficient of NaI. The phonon-assisted processes are dominated by the acoustic and the longitudinal optical (LO) phonon modes, while the contribution by the transverse optical (TO) phonons is approximately one order of magnitude smaller.

sampling grid of $30 \times 30 \times 30$ is sufficient to converge the Auger coefficients. The same figure also shows that the direct Auger coefficient does not depend sensitively on the band gap. For example, if the band gap changes within ± 0.3 eV from the experimental value (5.8 eV) the direct Auger coefficient changes by at most 50 %. The dependence of the direct Auger on the band gap follows the Arrhenius activation law derived for intraband Auger processes ($C \propto \exp(-E_A/k_B T)$), where the activation energy E_A is proportional to the gap.[27,28] As we discuss below in the analysis of the temperature dependence, the direct Auger coefficient of NaI follows this activation law (although AR in NaI occurs through interband processes to higher conduction bands) with an activation energy ($E_A = 0.18$ eV) that is only a small fraction (3.1 %) of the band gap.

The phonon-assisted AR coefficients are shown in Fig. 4 as a function of the band gap. The value of the phonon-assisted Auger coefficient at the experimental band gap ($5.6 \pm 0.3 \times 10^{-32}$ cm^{6}s^{-1}) is approximately two orders of magnitude larger than the direct one and therefore phonon-assisted processes dominate AR in NaI. This value is also comparable to phonon-assisted e-e-h AR values in semiconductors such as GaN (4×10^{-32} cm^{6}s^{-1})[13] and GaAs (1.1×10^{-31} cm^{6}s^{-1}).[14] Figure 5 shows the contribution of the various phonon modes to the phonon-assisted Auger coefficient. AR in NaI is mediated primarily by the acoustic and the longitudinal optical (LO) phonons, while the contribution by the transverse optical (TO) modes is approximately one order of magnitude smaller. Figure 6 shows the phonon-assisted Auger results analyzed in terms of the contribution by the various phonon wave vectors. The results indicate that the dominant contributions occur at wave vectors
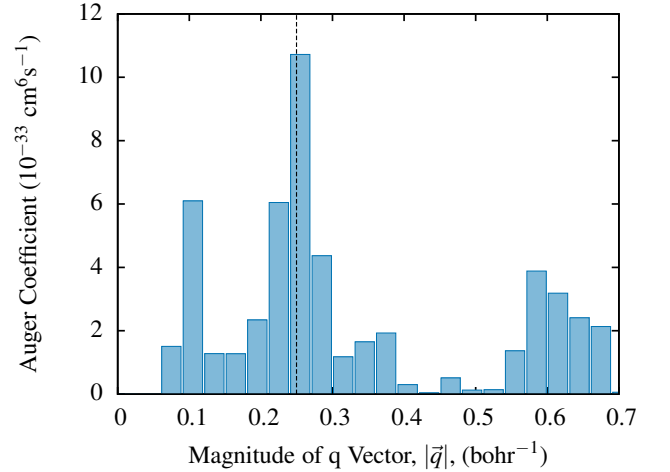

FIG. 6. The distribution of the contribution by the various phonon wave vectors to the phonon-assisted Auger coefficient of NaI. The vertical line represents the edge of the BZ.

comparable to the BZ dimensions that correspond to phonon wavelengths comparable to the lattice constant. Therefore, AR in NaI is primarily assisted by short-range phonon scattering.

Comparing with the coefficients fitted to experimental data, we first note that our calculated rate is several orders of magnitudes smaller than the value of 1.07×10^{-20} cm^{6}s^{-1} obtained by Bizarri *et al.*[8] We note however, that recently more improved sets of rate equations and boundary conditions have been developed.[16,17,29] Comparing to more recent results from fits ($C = 3.2 \times 10^{-29}$ cm^{6}s^{-1}) to z-scan experiments, our calculated values are off by a few decades.[16,17] This well illustrates the

difficulty in fitting a rate equation model to a very complex set of events and interdependent mechanisms. While one possible cause for the difference between our results and experimental data is thallium doping present in NaI samples that were studied in experiment, we note that Refs. 16 and 17 have considered both pristine and Tl-doped CsI with only a small variation (a factor of about 1.5) of the AR coefficients. We therefore expect that the inclusion of dopants does not have a large effect on the AR rate.

Interestingly, for a wide range of materials, Williams *et al.*, noted an empirical band-gap rule.[16,17] This trend was however not followed by the halide systems under consideration, which instead displayed values that exceeded the expected values by three to four orders of magnitude. The plausible explanation by the authors was the following: (*i*) the underlying model and assumptions are wrong or insufficient, or (*ii*) the excitation energy exceeds the band gap for at least NaI by about $0.3\,\text{eV}$ and might leave the carriers with very high electronic temperatures, or (*iii*) the Auger recombination might involve self-trapped holes (V_k-centers) with localized hole states in the forbidden gap. We note that our predicted value actually obeys the observed empirical band gap rule. To assess the effect of high electronic temperature on AR coefficients, we performed direct AR calculations for increasing electronic temperatures up to 2500 K (Fig. 7). The high-temperature calculations were performed with a $14 \times 14 \times 14$ k point grid since the convergence with respect to mesh size is faster for higher temperatures. We further fitted the data for the experimental band gap of 5.8 eV with an Arrhenius activation law $C(T) = C_0 \exp(-E_A/k_B T)$ (inset of Fig. 7). The fit parameters are $C_0 = 2.95 \times 10^{-32}\text{cm}^6\text{s}^{-1}$ and $E_A = 0.18$ eV $= 0.031 E_g$. Using this model, we obtained changes in the direct AR coefficient of at most 50% if the band gap is changed by ± 0.3 eV as was found in the calculated data. We can extrapolate this model to infinite temperature and find that the maximum direct AR coefficient is C_0, which is still a factor of 2 lower than the phonon-assisted AR coefficient. Therefore phonon-assisted AR dominates over direct AR even at high electronic temperatures.

The third possibility of a self-trapped hole to participate in the Auger process is indeed very interesting, but it is beyond the scope of the present work. We note however that the localized nature of the hole level relaxes the momentum conservation selection rules and may lead to larger rates. Furthermore, it is also possible that the localized empty levels provide more routes for direct AR.

In summary, we performed first-principles calculations to find the direct and phonon-assisted AR coefficients for the basic scintillating material, sodium iodide. We found that the phonon-assisted process is dominant in NaI, and the magnitude of the AR coefficient is smaller than values derived in previous work. Understanding AR and resolving the discrepancy with previous modeling work is necessary to successfully model the scintillating process
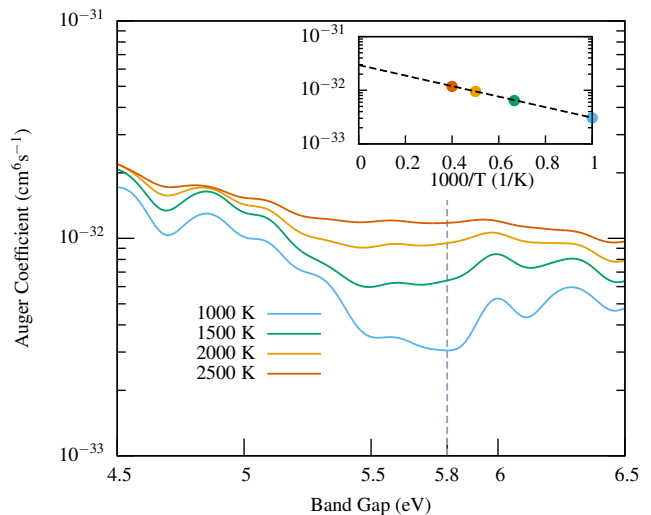

FIG. 7. The direct Auger recombination coefficient for varying electronic temperatures. The direct AR coefficient follows an Arrhenius activation-law model (inset), which predicts a maximum direct AR coefficient of $2.95 \times 10^{-32}\text{cm}^6\text{s}^{-1}$ that is less than the phonon-assisted coefficient.

in sodium iodide. Being able to better predict how this and other scintillating materials react during the high-energy impact would allow us to guide future materials design aimed at dramatically improving the device performance and developing detectors that easily allow radiation sources to be identified without error.

[1]R. Kouzes, in *Nuclear Renewable Energy Conference (INREC), 2010 1st International* (2010) pp. 1–3.

[2]"Combating nuclear smuggling: Lessons learned from cancelled radiation portal monitor program could help future acquisitions," Tech. Rep. GAO-13-37 (U.S. General Accountability Office, 2012).

[3]P. Dorenbos, Phys. Status Solidi A **202**, 195 (2005).

[4]A. V. Vasil'ev, IEEE Trans. Nucl. Sci. **55**, 1054 (2008).

[5]W.-S. Choong, G. Hull, W. W. Moses, K. Vetter, S. Payne, N. Cherepy, and J. Valentine, Nuclear Science, IEEE Transactions on **55**, 1073 (2008).

[6]S. Kerisit, K. M. Rosso, B. D. Cannon, F. Gao, and Y. Xie, J. Appl. Phys. **105**, 114915 (2009).

[7] G. Bizarri, W. Moses, J. Singh, A. Vasilev, and R. Williams, Journal of Luminescence **129**, 1790 (2009), special Issue based on The 15th International Conference on Luminescence and Optical Spectroscopy of Condensed Matter (ICL'08).

[8] G. Bizarri, N. Cherepy, W. S. Choong, G. Hull, W. Moses, S. Payne, J. Singh, J. Valentine, A. N. Vasilev, and R. Williams, IEEE Transactions on Nuclear Science **56**, 2313 (2009).

[9] W. W. Moses, S. A. Payne, W.-S. Choong, G. Hull, and B. W. Reutter, IEEE Transactions on Nuclear Science **55**, 1049 (2008).

[10] S. Payne, W. W. Moses, S. Sheets, L. Ahle, N. Cherepy, B. Sturm, S. Dazeley, G. Bizarri, and W.-S. Choong, IEEE Trans. Nucl. Sci. **58**, 3392 (2011).

[11] W. W. Moses, G. A. Bizarri, R. T. Williams, S. A. Payne, A. N. Vasil'ev, J. Singh, Q. Li, J. Q. Grim, and W.-S. Choong, Ieee Transactions on Nuclear Science **59**, 2038 (2012).

[12] B. K. Ridley, *Quantum Processes in Semiconductors* (Clarendon Press, Oxford, 1982).

[13] E. Kioupakis, P. Rinke, K. T. Delaney, and C. G. Van de Walle, Appl. Phys. Lett. **98**, 161107 (2011).

[14] D. Steiauf, E. Kioupakis, and C. G. Van de Walle, ACS Photonics **0**, null (0), http://pubs.acs.org/doi/pdf/10.1021/ph500119q.

[15] Y. C. Shen, G. O. Mueller, S. Watanabe, N. F. Gardner, A. Munkholm, and M. R. Krames, Applied Physics Letters **91**, 141101 (2007).

[16] R. T. Williams, J. Q. Grim, Q. Li, K. B. Ucer, G. A. Bizarri, S. Kerisit, F. Gao, P. Bhattacharya, E. Tupitsyn, E. Rowe, V. M. Buliga, and A. Burger, "Experimental and computational results on exciton/free-carrier ratio, hot/thermalized carrier diffusion, and linear/nonlinear rate constants affecting scintillator proportionality," (2013).

[17] J. Q. Grim, K. B. Ucer, A. Burger, P. Bhattacharya, E. Tupitsyn, E. Rowe, V. M. Buliga, L. Trefilova, A. Gektin, G. A. Bizarri, W. W. Moses, and R. T. Williams, Physical Review B **87**, 125117 (2013).

[18] J. P. Perdew, K. Burke, and M. Ernzerhof, Phys. Rev. Lett. **77**, 3865 (1996).

[19] J. Ihm, A. Zunger, and M. L. Cohen, Journal of Physics C: Solid State Physics **12**, 4409 (1979).

[20] N. Troullier and J. L. Martins, Phys. Rev. B **43**, 1993 (1991).

[21] P. Giannozzi, S. Baroni, N. Bonini, M. Calandra, R. Car, C. Cavazzoni, D. Ceresoli, G. L. Chiarotti, M. Cococcioni, I. Dabo, A. D. Corso, S. de Gironcoli, S. Fabris, G. Fratesi, R. Gebauer, U. Gerstmann, C. Gougoussis, A. Kokalj, M. Lazzeri, L. Martin-Samos, N. Marzari, F. Mauri, R. Mazzarello, S. Paolini, A. Pasquarello, L. Paulatto, C. Sbraccia, S. Scandolo, G. Sclauzero, A. P. Seitsonen, A. Smogunov, P. Umari, and R. M. Wentzcovitch, J. Phys.: Condens. Matter **21**, 395502 (2009).

[22] P. Rodnyi, *Physical Processes in Inorganic Scintillators* (CRC Press Inc, 1997).

[23] N. Marzari, A. A. Mostofi, J. R. Yates, I. Souza, and D. Vanderbilt, Rev. Mod. Phys. **84**, 1419 (2012).

[24] A. A. Mostofi, J. R. Yates, Y.-S. Lee, I. Souza, D. Vanderbilt, and N. Marzari, Comput. Phys. Commun. **178**, 685 (2008).

[25] E. Kioupakis, Q. Yan, D. Steiauf, and C. G. V. de Walle, New Journal of Physics **15**, 125006 (2013).

[26] G. Cappellini, R. Del Sole, L. Reining, and F. Bechstedt, Physical Review B **47**, 9892 (1993).

[27] H. Frhlich and J. O'Dwyer, Proceedings of the Physical Society. Section A **63**, 81 (1950).

[28] A. R. Beattie and P. T. Landsberg, Proceedings of the Royal Society of London. Series A. Mathematical and Physical Sciences **249**, 1629 (1959).

[29] Q. Li, X. Lu, and R. T. Williams, "Toward a user's toolkit for modeling scintillator non-proportionality and light yield," (2014).